

# Dual Coding Concatenation for Burst-Error Correction in Probabilistic Amplitude Shaping

Skvortcov, Pavel; Koike-Akino, Toshiaki; Millar, David S.; Kojima, Keisuke; Parsons, Kieran

TR2021-111 September 16, 2021

## Abstract

We investigate a dual coding concatenation in probabilistic amplitude shaping to mitigate the impact of post-shaping burst errors. We show that the joint use of pre-/post-shaping BCH codes can reduce the required input bit error rate (BER) for a short-length shaping system.

*European Conference on Optical Communication (ECOC) 2021*

© 2021 MERL. This work may not be copied or reproduced in whole or in part for any commercial purpose. Permission to copy in whole or in part without payment of fee is granted for nonprofit educational and research purposes provided that all such whole or partial copies include the following: a notice that such copying is by permission of Mitsubishi Electric Research Laboratories, Inc.; an acknowledgment of the authors and individual contributions to the work; and all applicable portions of the copyright notice. Copying, reproduction, or republishing for any other purpose shall require a license with payment of fee to Mitsubishi Electric Research Laboratories, Inc. All rights reserved.



# Dual Coding Concatenation for Burst-Error Correction in Probabilistic Amplitude Shaping

Pavel Skvortcov<sup>(1,2)</sup>, Toshiaki Koike-Akino<sup>(1)</sup>, David S. Millar<sup>(1,3)</sup>, Keisuke Kojima<sup>(1)</sup>, Kieran Parsons<sup>(1)</sup>

<sup>(1)</sup> Mitsubishi Electric Research Laboratories (MERL), Cambridge, MA 02139, USA. [koike@merl.com](mailto:koike@merl.com)

<sup>(2)</sup> Aston University, Birmingham, B4 7ET, UK.

<sup>(3)</sup> Infinera Corporation, San Jose, CA 95119, USA.

**Abstract** We investigate a dual coding concatenation in probabilistic amplitude shaping to mitigate post-shaping burst errors. The joint use of pre-/post-shaping BCH codes can significantly relax bit error rate (BER) threshold after soft-decision code resulting in signal-to-noise ratio (SNR) gain of 0.1 dB.

## Introduction

Widely studied probabilistic amplitude shaping (PAS)<sup>[1]</sup> has become a realizable technology<sup>[2]</sup>. Many practical shaping approaches<sup>[3]–[7]</sup> were proposed to demonstrate the advantage of short-length shaping for nonlinear optical channels, in favour of reduced hardware complexity. For the advanced sphere shaping, the optimal shaping length is in the range of 100–200 amplitudes for long-haul links<sup>[7],[8]</sup> and 20–50 amplitudes for highly nonlinear short-distance links<sup>[6],[9],[10]</sup>.

For PAS architecture, which typically employs *reverse* concatenation of shaping and forward error correction (FEC) stages, FEC coding is performed on shaped bits. At the receiver, shaped bits are first decoded with FEC and then demapped (i.e., de-shaped) to information bits under the assumption that all bits are correctly decoded. While FEC systems can achieve arbitrarily low output bit error rates (BERs), they always have a non-zero probability of errors in practice.

The commonly considered threshold on acceptable performance after FEC decoding is a BER of  $10^{-15}$ . However, for systems utilizing PAS architecture BER enhancement may occur due to shaping demapping. A single bit error within a shaped sequence (of length  $L_{Sh}$  bits) at the input to a shaping demapper in most cases will cause a burst error of length  $L_{Sh}$  after demapping. While some shaping demappers were studied to mitigate BER enhancement<sup>[11],[12]</sup>, it is not universally applicable to all mapping/demapping schemes.

One approach to mitigate BER enhancement in PAS is to use a *dual concatenation* with pre- and post-shaping FEC layers. We propose a low-complexity scalable architecture for correction of burst errors in pre-shaping FEC layer,

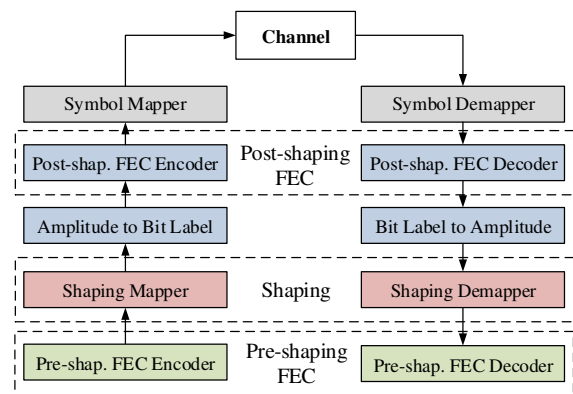


**Fig. 1:** Dual concatenated PAS architecture with post-shaping inner and pre-shaping outer FEC layers.

which is based on parallel Bose–Chaudhuri–Hocquenghem (BCH) codes. We analytically verify the significant gain of the proposed dual concatenation approach over the conventional reverse concatenation for PAS systems using 64-ary quadrature-amplitude modulation (QAM).

## Dual Concatenation for PAS

Fig. 1 depicts the proposed PAS with pre- and post-shaping FEC layers. This architecture is based on a joint forward and reverse concatenation of the shaping and FEC (i.e., shaping precedes FEC coding in reverse concatenation, while opposite in forward concatenation).

The shaping rate (in bits per unsigned amplitude, b/Amp) is defined as

$$R_{Sh} = \frac{L_{DeSh}}{L_{Sh}^{Amp}} = \frac{L_{DeSh}}{L_{Sh}}(m - 1), \quad (1)$$

where  $L_{Sh}^{Amp}$  is the length of shaped sequence in amplitudes,  $L_{Sh}$  is the length of shaped sequence in bits,  $L_{DeSh}$  is the length of de-shaped sequence in bits, and  $m$  is the number of bits per amplitude (i.e.,  $m = \log_2 M$  for  $M$ -ary amplitudes).

For post-shaping FEC, we assume a concatenation of powerful soft-decision (SD) low-density

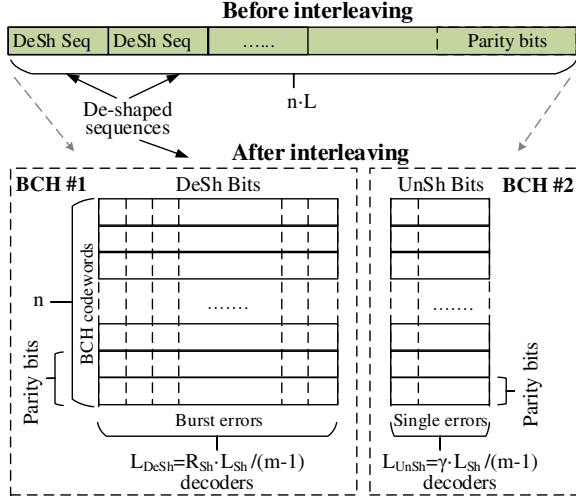


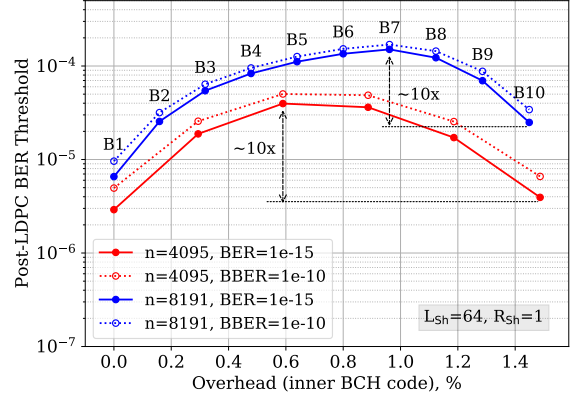
Fig. 2: Parallel structure for pre-shaping BCH code.

parity-check (LDPC) code and low-complexity BCH code. The total code rate of post-shaping inner FEC is  $R_{\text{FEC}}^{\text{PostSh}} = R_{\text{SD}}^{\text{PostSh}} \cdot R_{\text{BCH}}^{\text{PostSh}} = (m-1+\gamma)/m$ , where  $0 \leq \gamma \leq 1$  specifies the portion of unshaped bits (information bits that are carried on signs of amplitudes in addition to parity bits). The size of unshaped bits is  $L_{\text{UnSh}} = \gamma L_{\text{Sh}}/(m-1)$  and that of parity bits is  $L_{\text{Par}} = (1-\gamma)L_{\text{Sh}}/(m-1)$ .

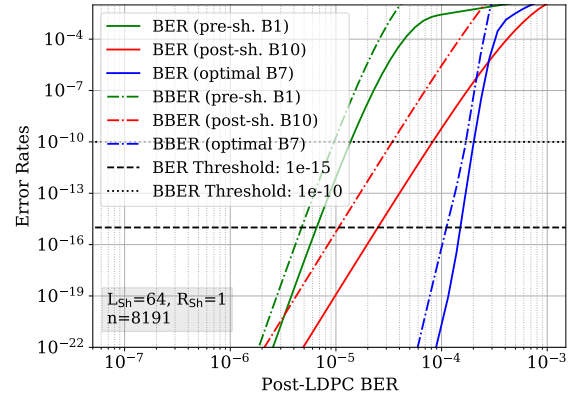
For pre-shaping FEC, we consider parallel BCH structure as shown in Fig. 2. Block interleaving is used to spread the burst errors among multiple BCH codewords (each column in interleaved structure is a codeword). For the burst of length  $l$ , we can use the code of length  $n = n'/L$  with error correcting ability of  $l/L$  with  $L$ -way interleaving. We note that this structure enables fully parallel encoding/decoding, suited for high-throughput systems.

This structure can be easily scaled with shaping rate. We assume that parallel structure is initially designed for the maximum shaping rate (i.e.,  $L_{\text{DeSh}} = L_{\text{Sh}}$ ). Then, adaptivity is achieved by subsequently disabling some of parallel encoders/decoders. Also, for shaped and unshaped bits separate BCH codes can be used, since the requirement for error correcting ability can be different — for unshaped bits there is no BER enhancement and, hence, a BCH code with reduced error correcting ability can be used to minimize the overall overhead.

The transmission rate (in bits per 1D-symbol, b/1D) of PAS systems with pre-shaping FEC is expressed as  $R_{\text{Tr}} = R_{\text{Sh}} \cdot R_{\text{BCH}}^{\text{PreSh}} + \gamma \cdot R_{\text{BCH}}^{\text{PreSh}'}$ , where  $R_{\text{BCH}}^{\text{PreSh}}$  is the rate of the pre-shaping BCH code for shaped bits,  $R_{\text{BCH}}^{\text{PreSh}'}$  is the rate of the pre-shaping BCH code for unshaped bits.



(a) Post-LDPC BER Threshold



(b) Output BER/BBER

Fig. 3: Optimal dual concatenation of inner and outer codes.

We note that pre-shaping coding is performed on shorter bit sequences compared to post-shaping coding (due to shaping/de-shaping), which can result in complexity reduction. Furthermore, in general, post-shaping coding is less efficient compared to pre-shaping coding, since not of the full alphabet of bit sequences of length  $L_{\text{Sh}}$  is utilized for signalling, however, coding protects all possible sequences of that length which results in extra parity bits and increased overhead.

### Performance Analysis

We analytically evaluate the performance of post- and pre-shaping BCH codes. We consider a PAS system with 64-QAM ( $m=3$ ) and a post-shaping LDPC code with a rate of  $R_{\text{LDPC}}^{\text{PostSh}} = 0.72$ . As per-

Tab. 1: Code parameters:  $n = 8191$

Configuration	$\text{OH}_{\text{BCH}}^{\text{PostSh}}$	$\text{OH}_{\text{BCH}}^{\text{PreSh}}$	$\text{OH}_{\text{BCH}}^{\text{PreSh}'}$	$R_{\text{Tr}}, \text{b/1D}$
B1 (pre-sh.)	0.00	2.77	2.44	1.1292
B2	0.16	2.44	2.27	1.1293
B3	0.32	2.27	1.12	1.1292
B4	0.48	1.94	0.96	1.1292
B5	0.64	1.61	0.80	1.1293
B6	0.80	1.29	0.64	1.1293
B7 (optimal)	0.96	0.96	0.48	1.1292
B8	1.12	0.48	0.48	1.1306
B9	1.29	0.16	0.16	1.1308
B10 (post-sh.)	1.45	0.00	0.00	1.1291

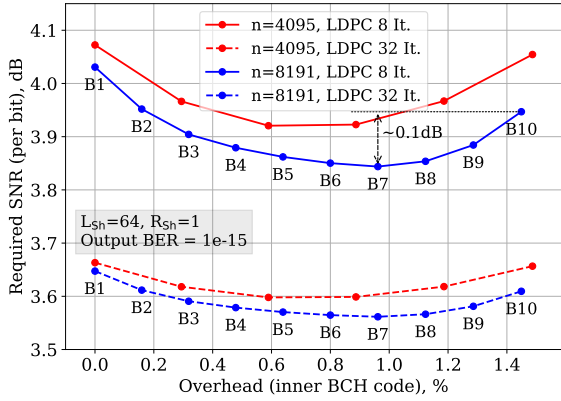


Fig. 4: Required SNR for post-shaping LDPC code.

formance metrics, we consider a post-LDPC BER threshold, which is a required BER after post-shaping LDPC code and a required SNR (per bit) at the input of LDPC code for a target system performance. For the target system performance, we use either a BER of  $10^{-15}$  or a background block error rate (BBER)<sup>[13]</sup> of  $10^{-10}$ . For BBER evaluation, we assume optical transport unit C1 (OTUC1) framing<sup>[14]</sup>.

Fig 3 shows the performance for various concatenation options of inner and outer BCH codes. The lengths of BCH codes are  $n = 4095$  and  $n = 8191$ . The total overhead for BCH codes is adjusted around 1.5 %, shaping rate is  $R_{Sh} = 1$  b/Amp, and shaping length is  $L_{Sh} = 64$ . We varied the overhead for post-shaping BCH code and defined complimentary overheads for pre-shaping BCH codes such that the transmission rate is closely matched with the case of post-shaping BCH only (i.e., conventional reverse concatenation). The overhead adjustment for  $n = 8191$  is listed in Table 1.

In Fig 3(a), left- and right-end points represent post-shaping BCH only and pre-shaping BCH only configurations, respectively, while points in the middle represent dual-coding concatenation. Comparing end points, we can observe that post-shaping BCH configuration slightly outperforms pre-shaping BCH configuration, especially for longer codes. With the optimal dual-BCH concatenation, the post-LDPC BER threshold can be improved approximately by an order of magnitude compared to only inner BCH configuration — from  $3 \times 10^{-6}$  to  $3 \times 10^{-5}$  for  $n = 4095$  and from  $2 \times 10^{-5}$  to  $2 \times 10^{-4}$  for  $n = 8191$  for target output BER of  $10^{-15}$ . Similar trends are observed for target output BBER of  $10^{-10}$ .

Fig. 3(b) shows overall output system error rates as a function of post-LDPC BER for post-shaping BCH only, pre-shaping BCH only, and op-

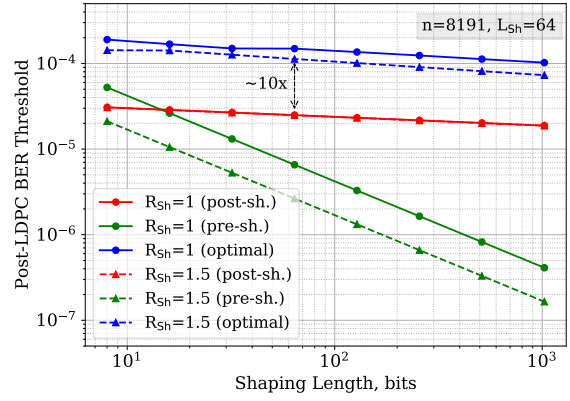


Fig. 5: Impact of shaping length.

timal dual-BCH concatenation. We can see that the gain of the proposed dual concatenation is more significant for a system which requires more stringent BER/BBER target.

For required SNR analysis, we consider a state-of-the-art post-shaping SD FEC using an LDPC code with a rate of 0.72, a length of 13,200, and a layered sum-product decoding over 8 or 32 iterations. Fig. 4 shows required SNR (per bit) for a target system BER of  $10^{-15}$ . For 8-iteration decoding, the SNR gain is greater than 0.1 dB, while for 32 iterations the gain is around 0.05 dB.

Fig. 5 shows the impact of shaping length. We consider two shaping rates of  $R_{Sh} = 1$  and  $R_{Sh} = 1.5$ , for a shaping length from  $L_{Sh} = 8$  to 1024 (equivalently, from  $L_{Sh}^{Amp} = 4$  to 512). Note that the performance of post-shaping BCH codes does not depend on the shaping rates. For short-length shaping, pre-shaping BCH is comparable to post-shaping BCH (slightly superior for  $R_{Sh} = 1$ ), while for long-length shaping the pre-shaping BCH is considerably worse. Nevertheless, the joint use of pre- and post-shaping BCH codes can significantly improve the performance regardless of the shaping length.

## Discussion and Conclusions

We have analyzed the dual coding concatenation for PAS using parallel BCH codes for pre-shaping and post-shaping FEC layers. This architecture offers flexibility for shaping rate adaptation and potentially reduced implementation complexity.

For short-length shaping, pre-shaping coding can provide similar performance to that of the standard reverse concatenation. More importantly, optimally concatenated dual-coding configuration can significantly relax the post-LDPC BER threshold by an order of magnitude, which can result in 0.1 dB required SNR improvement considering the use of state-of-the-art LDPC code.

## References

- [1] G. Böcherer, F. Steiner, and P. Schulte, "Bandwidth efficient and rate-matched low-density parity-check coded modulation", *IEEE Transactions on Communications*, vol. 63, no. 12, pp. 4651–4665, 2015.
- [2] H. Sun, M. Torbatian, M. Karimi, R. Maher, S. Thomson, M. Tehrani, Y. Gao, A. Kumpera, G. Soliman, A. Kakkar, M. Osman, Z. A. El-Sahn, C. Daggart, W. Hou, S. Sutarwala, Y. Wu, M. R. Chitgarha, V. Lal, H. Tsai, S. Corzine, J. Zhang, J. Osenbach, S. Buggaveeti, Z. Morbi, M. I. Olmedo, I. Leung, X. Xu, P. Samra, V. Dominic, S. Sanders, M. Ziari, A. Napoli, B. Spinnler, K. Wu, and P. Kandappan, "800G DSP ASIC design using probabilistic shaping and digital sub-carrier multiplexing", *IEEE/OSA Journal of Lightwave Technology*, vol. 38, no. 17, pp. 4744–4756, 2020.
- [3] P. Schulte and G. Böcherer, "Constant composition distribution matching", *IEEE/OSA Journal of Lightwave Technology*, vol. 62, no. 1, pp. 430–434, 2016.
- [4] D. S. Millar, T. Fehenberger, T. Koike-Akino, K. Kojima, and K. Parsons, "Distribution matching for high spectral efficiency optical communication with multiset partitions", *IEEE/OSA Journal of Lightwave Technology*, vol. 37, no. 2, pp. 517–523, 2019.
- [5] T. Fehenberger, D. S. Millar, T. Koike-Akino, K. Kojima, and K. Parsons, "Multiset-partition distribution matching", *IEEE Transactions on Communications*, vol. 67, no. 3, pp. 1885–1893, 2019.
- [6] P. Skvortcov, I. Phillips, W. Forsyia, T. Koike-Akino, K. Kojima, K. Parsons, and D. S. Millar, "Nonlinearity tolerant LUT-based probabilistic shaping for extended-reach single-span links", *IEEE Photonics Technology Letters*, vol. 32, no. 16, pp. 967–970, 2020.
- [7] A. Amari, S. Goossens, Y. C. Gültekin, O. Vassilieva, I. Kim, T. Ikeuchi, C. M. Okonkwo, F. M. J. Willems, and A. Alvarado, "Introducing enumerative sphere shaping for optical communication systems with short block-lengths", *IEEE/OSA Journal of Lightwave Technology*, vol. 37, no. 23, pp. 5926–5936, 2019.
- [8] S. Goossens, S. Van der Heide, M. Van den Hout, A. Amari, Y. C. Gültekin, O. Vassilieva, I. Kim, T. Ikeuchi, F. M. J. Willems, A. Alvarado, and C. Okonkwo, "First experimental demonstration of probabilistic enumerative sphere shaping in optical fiber communications", in *Proc. Opto-Electron. Commun. Conf. (OECC) and Int. Conf. on Phot. in Switch. and Comp. (PSC)*, 2019.
- [9] O. Geller, R. Dar, M. Feder, and M. Shttaif, "A shaping algorithm for mitigating inter-channel nonlinear phase-noise in nonlinear fiber systems", *IEEE/OSA Journal of Lightwave Technology*, vol. 34, no. 16, pp. 3884–3889, 2016.
- [10] P. Skvortcov, I. Phillips, W. Forsyia, T. Koike-Akino, K. Kojima, K. Parsons, and D. S. Millar, "Huffman-coded sphere shaping for extended-reach single-span links", *IEEE Journal of Selected Topics in Quantum Electronics*, vol. 27, no. 3, pp. 1–15, 2021.
- [11] T. Yoshida, M. Karlsson, and E. Agrell, "Hierarchical distribution matching for probabilistically shaped coded modulation", *IEEE/OSA Journal of Lightwave Technology*, vol. 37, no. 6, pp. 1579–1589, 2019.
- [12] —, "Technologies toward implementation of probabilistic constellation shaping", in *In Proceedings of European Conference on Optical Communication (ECOC)*, 2018, pp. 1–3.
- [13] OTU-T, *Error performance parameters and objectives for multioperator international paths within optical transport networks*. [Online]. Available: [www.itu.int/rec/T-REC-G.8201](http://www.itu.int/rec/T-REC-G.8201).
- [14] —, *Interfaces for the optical transport network*. [Online]. Available: [www.itu.int/rec/T-REC-G.709](http://www.itu.int/rec/T-REC-G.709).